Tectonophysics 769 (2019) 228185

Contents lists available at ScienceDirect

Tectonophysics

journal homepage: www.elsevier.com/locate/tecto

Repeating earthquakes and interplate coupling along the western part of the North Anatolian Fault

N. Uchida[a,*], D. Kalafat[b], A. Pinar[b], Y. Yamamoto[c]

[a] Graduate School of Science, Tohoku University, Aoba-ku, Sendai 980-8578, Japan
[b] Kandilli Observatory & Earthquake Research Institute, Boğaziçi University, Istanbul, Turkey
[c] Japan Agency for Marine-Earth Science and Technology, Yokohama 236-0001, Japan

ARTICLE INFO

Keywords:
Repeating earthquake
Fault creep
North Anatolian Fault
Earthquake relocation
Sea of Marmara

ABSTRACT

The Sea of Marmara accommodates segments of the North Anatolian Fault (NAF) in Turkey and remains the only part of the western NAF that has not ruptured during the last century. At its nearest, the segment is ~20 km from Istanbul, the largest city in Turkey. Thus, it is important to understand the locking state of the fault, since it illuminates the strain accumulation rate along the fault segments, which in turn is an important input parameter in seismic hazard studies. To infer the interplate locking state, we used repeating earthquakes that indicate fault creep in the surrounding area using long-term (April 2005 to May 2013) seismic observations at 12 broadband seismic stations operated by Bogazici University Kandilli Observatory and Earthquake Research Institute. We defined repeating earthquakes from waveform coherences that were > 0.95 for 40-second-long waveforms of the vertical component. Using the selection procedure, we found 21 repeating earthquakes with magnitude 2.3 to 3.2 that are grouped into 9 sequences. They are distributed along the main NAF, comprising three groups of activity, one group in the Sea of Marmara and a group either side to the east and west. The three groups are located near the boundary of previous large earthquake ruptures, suggesting relatively weak coupling there. We also estimated the fault creep rate from the cumulative slip of the repeating earthquakes using a scaling relationship between repeating earthquakes' moment and slip. The slip rate for these three groups are similar (3–4 cm/yr) and comparable to, albeit slightly higher than, those expected from global plate models (~2.4 cm/yr). This suggests relatively weak locking around the groups. The relocation results of the repeating earthquake hypocenters in the Sea of Marmara suggest the creep is occurring at 10 to 20 km depth. These results suggest heterogeneous coupling in the segment.

1. Introduction

The North Anatolian Fault (NAF) is a ~1200 km long strike-slip fault between the Eurasian and Anatolian plates, in Turkey. Regional and global plate models suggest right-lateral relative plate motion of 2.2–2.4 cm/yr across the plate boundary (e.g., McClusky et al., 2000; Sella et al., 2002). The seismic activity along the NAF has the unique attribute that the major earthquakes have migrated from east to west from 1939 to 1999 (e.g., Şengör et al., 2005; Stein et al., 1997) (Fig. 1). The Sea of Marmara segment, located to the south of Istanbul, the largest city in Turkey, is known as a segment of about 150 km that has not ruptured since 1766 and characterizing the seismic hazard in this area is very important (Bulut et al., 2011). To the east of the segment, 1999 Izmit earthquake (Mw 7.4) ruptured along a 100–150 km fault segment (Tibi et al., 2001; Barka et al., 2002; Bouchon et al., 2002) and to the west of the segment, the 1912 Mürefte (Ganos) earthquake (Mw 7.4) ruptured along a ~120 km fault segment (Aksoy et al., 2010) (Fig. 1). The seismic activity in the Sea of Marmara region over the last 2000 years suggests the segment can be divided to subsegments that produces M ~7 earthquakes, and there is no evidence of major earthquakes having ruptured the whole Sea of Marmara region simultaneously (Ambraseys, 2002). Beneath the Sea of Marmara, the probability of the occurrence of a M > 7 earthquake was estimated to be ~35–70% until 2034 assuming full locking at 0–12.5 km depth (Parsons, 2004). However, little is known about the interplate locking distribution for the segment under the Sea of Marmara.

Recently, sea bottom acoustic ranging was conducted across the fault trace at two places along the Marmara segment of NAF. They showed surface creep of 1.1 cm/yr (Yamamoto et al., 2019) and surface locking (Sakic et al., 2016) at Western High and Central High,

* Corresponding author.
E-mail address: naoki.uchida.b6@tohoku.ac.jp (N. Uchida).

https://doi.org/10.1016/j.tecto.2019.228185
Received 28 February 2019; Received in revised form 9 July 2019; Accepted 27 August 2019
Available online 27 August 2019

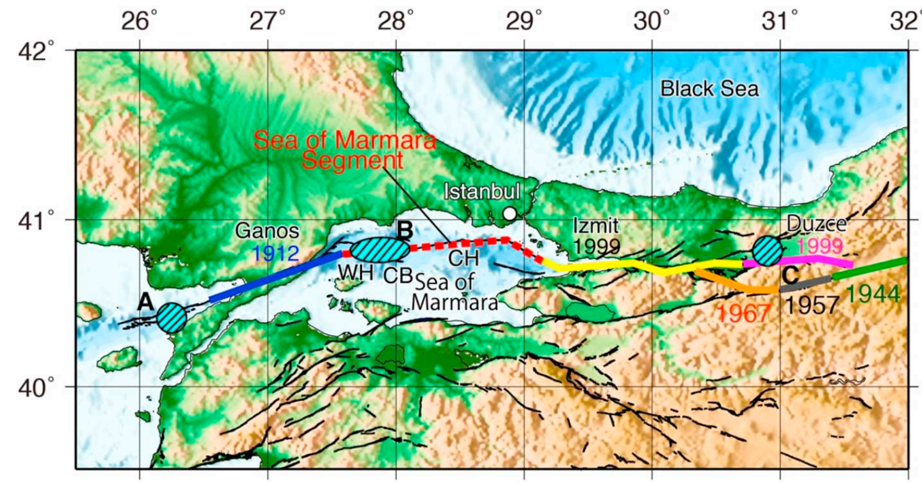

Fig. 1. Regional map around the Sea of Marmara with the fault trace along the North Anatolian Fault and previous rupture extents. WH, CB and CH denote Western High, Central Basin and Central High, respectively. Regions A - C show the locations of repeater sequences.

respectively (Fig. 1). Yamamoto et al. (2019) constructed a depth dependent locking model that has partial locking in the 0–8 km depth range, full locking in the 8–11 km depth range, and complete decoupling below 11 km. Sakic et al. (2016) showed that the creep rate in 6 months is < 0.6 cm/yr. These geodetic observations are important to constrain the locking state of the fault segment beneath the sea, but the locations of the observations are limited at two points along the fault and it is difficult to estimate the distribution of locking in a wide area along the NAF beneath the Sea of Marmara.

Seismicity data contain additional information to infer fault coupling over larger spatial extents than that from surface acoustic ranging observations when the hypocenter location is accurately determined. In the western part of the Sea of Marmara, Yamamoto et al. (2017) found ~10 km difference in the maximum depth of shallow seismicity along western part of NAF based on ocean-bottom seismometer data. Their relocation has ~0.2 km accuracy and found a seismically inactive area in the western part. They attributed this gap to a locking patch. In the eastern part of the Sea of Marmara, Bohnhoff et al. (2013) found a lack of earthquakes at the depths of 0–10 km based on seismic observations that include island stations close to the fault trace and suggested fault locking in this depth range. However, we have to note that these are not direct observations of fault creep on the NAF. On the other hand, repeating earthquakes provide direct evidence for fault creep (e.g., Uchida and Bürgmann, 2019). Schmittbuhl et al. (2016) found 9 repeating earthquake sequences with relatively short recurrence intervals (~8 months) for 2008–2015 at the Central Basin in the Sea of Marmara (Fig. 1). They used 1–10 Hz band for waveform filtering which is low when considering the small size of target events (1 < M < 2.5) and have a possibility to include non-overlapping events (Uchida, 2019). Bohnhoff et al. (2017) found two repeating earthquake sequences at the Central Basin and Western High (Fig. 1). They used enough high frequency band (3–23 Hz) for relatively large events (M > 2.2). However, their search is limited in 5 subareas and period of 4 years. Therefore, it is important to identify repeating earthquakes which can definitely attributed to a recurrent rupture of the same area in a wider spatial and temporal ranges.

To this end, it is important to estimate fault creep distribution which can contribute the improvement of input parameter in seismic hazard studies. In this study, we selected repeating earthquakes from 8-year observations of seismic data to infer the locations where the fault creep is occurring.

2. Repeating earthquake analyses

2.1. Selection of repeating earthquakes and estimation of fault creep

Repeating earthquakes that share the same fault area are considered to represent repeated rupture of the same fault patch due to fault creep in the surrounding area. The repeating earthquakes represent the existence of fault creep and the spatio-temporal change can be estimated from the activity (e.g., Nadeau and McEvilly, 1999; Uchida and Bürgmann, 2019). They can be selected by the waveform similarity or precise locations based on hypocenter determinations. We used a similar method to that previously used for selecting repeating earthquakes in the northeastern Japan subduction zone (Uchida et al., 2006) and applied it to the earthquakes in Turkey. We used 12 broadband seismic stations operated by Bogazici University Kandilli Observatory and Earthquake Research Institute (KOERI) for the period from April 2005 to May 2013 (Fig. 2). The stations are selected to have long observation period and good spatial coverage along the western part of the NAF. The waveforms were windowed for 40 s starting 2 s before the P wave onset to 40 s after, while the waveform coherence was calculated for all event pairs with < 20 km horizontal separation by the KOERI hypocenter catalogue. The criterion for similarity was set such that the coherence must be > 0.95 for the 2–10 Hz band. For a robust detection based on relatively sparse stations, we defined repeating earthquake pair if one station fulfilled the criterion. To select continuously occurring sequences that are most likely to represent fault slow slip, we selected pairs with intervals > 1 year. A pair (group) of repeaters was then linked with another if the two pairs (groups) shared the same earthquake. This grouping procedure was iterated. The search included a total of about 10,400 shallow (0.2 km ≦ depth ≦ 46 km) earthquakes with magnitudes of 1.0 to 5.4.

The cumulative slip on the repeating earthquakes can be estimated using an empirical relationship between seismic moment (M_0) and slip (d). If a fault patch always slips seismically or the ratio of the seismic slip to the total slip on the patch is constant, the cumulative quasi-static slip (creep) in the area surrounding the patch can be estimated from the cumulative slip of the repeating earthquakes occurring on the patch.

In this study, we calculated the cumulative slip of repeating earthquakes using the following relationship proposed by Nadeau and Johnson (1998):

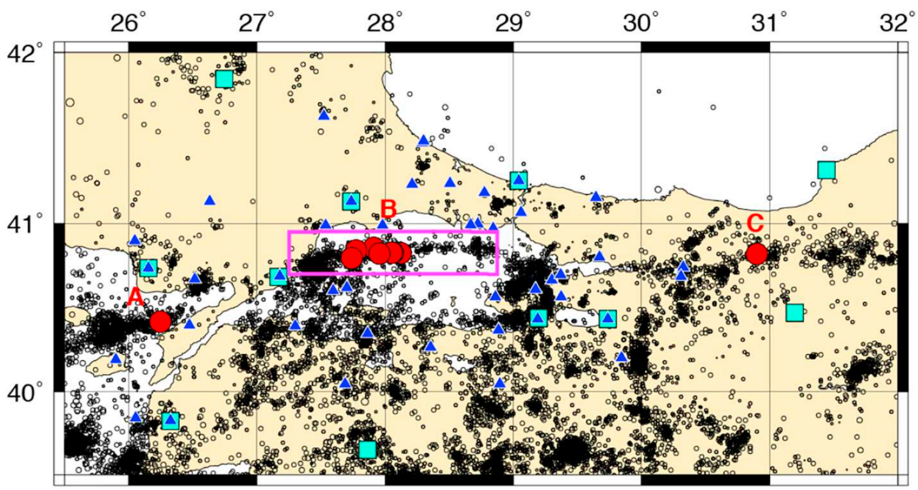

Fig. 2. The distribution of repeating earthquake sequences (red circles) and regular earthquakes (black dots) for the period from April 2005 to May 2013 based on KOERI hypocenter catalogue. The magenta rectangle shows the area for a detailed study (Figs. 4 and 6). Squares and triangles are stations used to select repeating earthquakes and relocate the earthquakes in the magenta rectangle, respectively. The stations used for hypocenter relocation (triangles) in the rectangle are not shown here but shown in Fig. 6.

$$\log(d) = -2.36 + 0.17\log(M_0) \quad (1)$$

where d is given in cm and M_0 is in dyne·cm.

The scalar moment for each event can be estimated from the magnitude determined by KOERI using the following relationship between magnitude (M) and scalar moment (Hanks and Kanamori, 1979):

$$\log(M_0) = 1.5M + 16.1 \quad (2)$$

2.2. The distribution of repeating earthquakes and their slip rates

The repeating earthquakes identified in this study are shown by red circles in Fig. 2 and listed in Table 1. We found 21 repeating earthquakes which are grouped into 9 sequences. The range in magnitude is 2.3 to 3.2 (Table 1). Although there are many regular earthquakes (black in Fig. 2), the repeating earthquakes are limited. We found three clusters of repeating earthquakes—to the west of the Sea of Marmara (region A), in the Sea of Marmara (region B), and to the east of the Sea of Marmara (region C) (Fig. 2). The maximum repeat times of the sequences are three that are located in region B. All these clusters are located along the NAF and in areas between fault segments (Fig. 1). They have very similar waveforms as shown in Fig. 3. Region A is located in an area of dense seismicity under the Aegean Sea (Fig. 2). There is only one sequence. The depth difference between the members of the sequence (Table 2) is probably due to poor depth constraint for the earthquakes. Region B in the Sea of Marmara has 7 sequences in the region and the detailed distribution of repeaters in the region show aligned distributions along the fault trace with a length of approximately 40 km along strike (Fig. 4). The depth differences for the earthquakes in the same region again show poor depth constraint for these earthquakes. Region C is located near the rupture boundary between the 1999 Izmit and Duzce earthquakes. This region has only one sequence.

The cumulative slip of repeating earthquakes in each region is shown in Fig. 5. It is notable that the cumulative slip for region B is averaged for 7 sequences. The cumulative slip is 27–30 cm in 8.2 years and the slip rate is 3.3–3.6 cm/yr for the three regions. For regions A and C in which we have only one sequence, we can also consider only the time interval between two earthquakes. By dividing the slip amount of the latter event by the interval the slip rate reduces to 2.1 cm/yr (corresponds to the gray lines in Fig. 5) for regions A and C. These variations in slip-rate estimate by the different time period considered

Table 1
List of repeating earthquakes. Please note the earthquake locations in group B show those relocated in this study.

Sequence number	Group	Date, minutes, sec	Latitude	Longitude	Depth (km)	Mag.	Largest coherence
1	B	201002241325.38	40.858	27.899	9.4	2.6	0.955
1	B	201212281209.30	40.851	27.924	9.7	2.3	0.955
2	B	200612230748.22	40.848	27.753	11.9	2.8	0.978
2	B	201002180456.12	40.830	27.750	16.3	2.8	0.978
3	C	200705020141.05	40.830	30.890	11.0	3.1	0.973
3	C	201303292254.08	40.810	30.911	8.0	2.8	0.973
4	B	200602121739.17	40.814	28.146	12.3	2.9	0.978
4	B	200911290921.25	40.815	28.120	8.3	2.8	0.978
5	B	201101150751.33	40.827	28.057	10.0	2.7	0.985
5	B	201304241624.20	40.821	28.049	14.8	2.6	0.985
6	B	200605210240.17	40.799	28.054	17.9	3.1	0.988
6	B	200812271925.07	40.828	28.040	8.0	3.2	0.988
6	B	201108041652.19	40.817	28.048	12.0	3.0	0.967
7	B	200808121840.48	40.824	27.950	13.0	3.1	0.987
7	B	201201020655.54	40.834	27.938	16.4	2.6	0.987
7	B	201301182118.56	40.814	27.938	18.5	2.5	0.977
8	B	200610141824.03	40.811	27.713	12.4	2.7	0.959
8	B	201107270921.49	40.819	27.716	15.8	2.8	0.951
8	B	201108112013.10	40.800	27.722	10.5	2.7	0.959
9	A	200705290307.03	40.420	26.240	18.0	3.1	0.964
9	A	201304201947.25	40.418	26.248	9.5	2.8	0.964

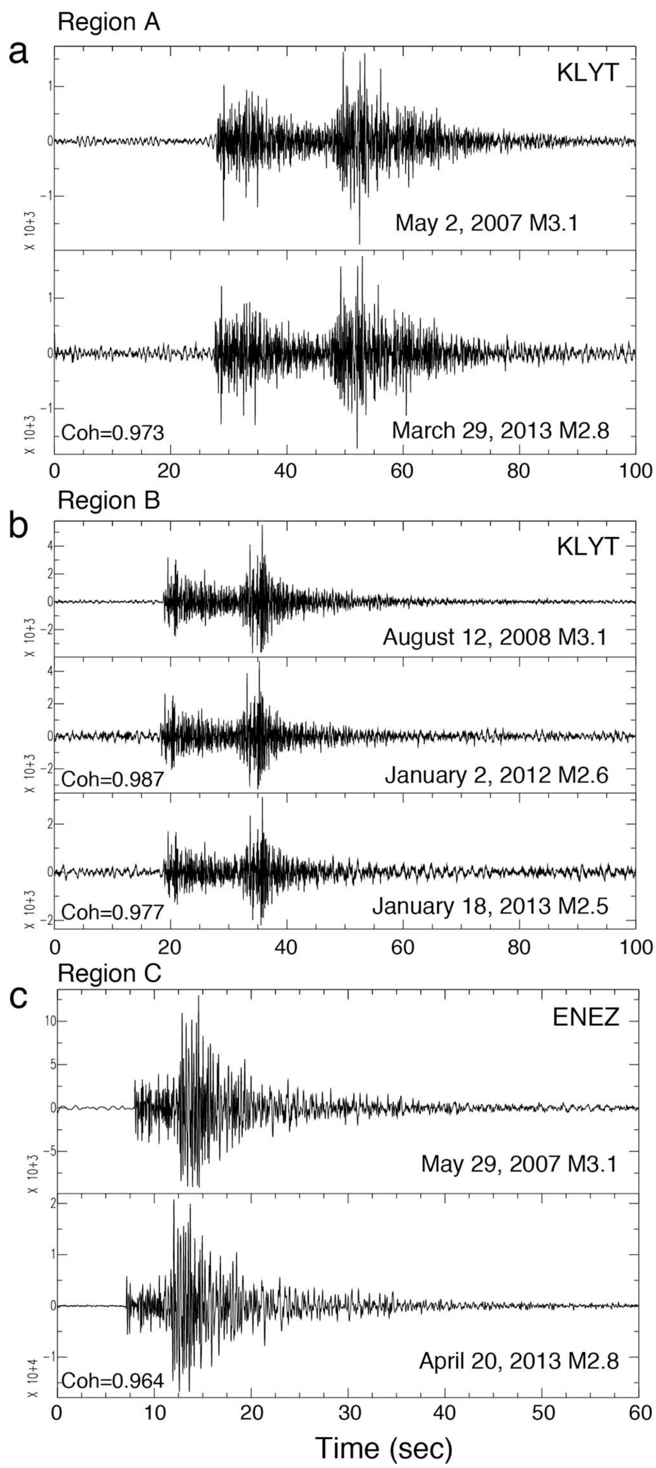

Fig. 3. The waveforms of repeating earthquakes in regions A to C. The origin times and magnitudes are shown at right bottom. The stations are shown at right top. The coherence value with top trace is shown in the left bottom of each panel.

for regions A and C show the rough variability of slip rate estimation by a single sequence. Region B, which has a relatively large number of sequences shows that there is a small temporal change in the slip rate during the period. Fig. 4 shows the slip rate for each sequence belonging to region B that is estimated from averaged interval and slip amount. They show the slip rate does not exhibit much variation among the sequences in region B.

Table 2
Comparison of the slip rate estimates from different studies. The average slip shows the slip amount of the repeating earthquakes averaged for the members within each sequence. The long-term rate is the deformation rate that is used to estimate the coupling ratio in each study.

Reference	Repeater magnitude	Period (years)	Slip estimation method	Average slip (mm)	Slip rate (mm/yr)	Recurrence interval (months)	Long-term rate (mm/yr)	Coupling ratio (%)
Schmittbuhl et al., 2016	M0.8–2.7	7.3	Spectrum analysis	0.3–2.5	0.5–4.0	~8	23	> 90
Bohnhoff et al., 2017	M2.7 and 2.8	4.0	Crack model (3 MPa stress drop)	10–15	4.7–10	12 and 38	15–20	25–75
This study	M2.3–3.2	8.2	Nadeau and Johnson (1998)	130–147	33–57	12–72	24	~0

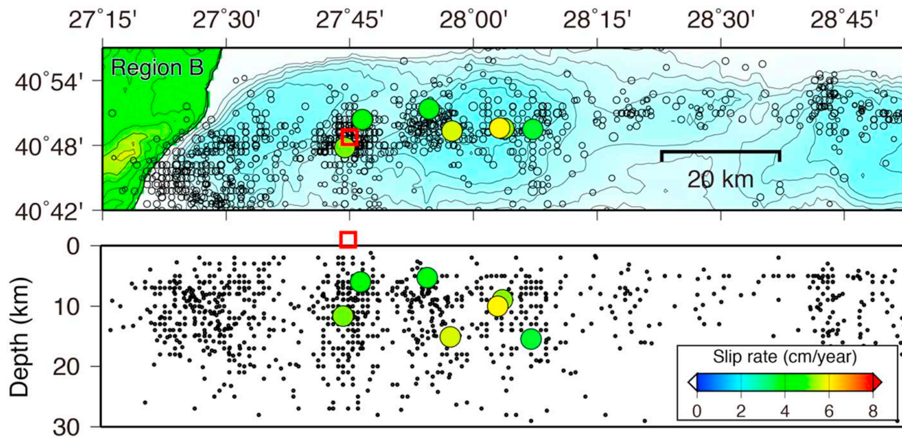

Fig. 4. Detailed map view and east-west cross section of region B. Colors show slip rate estimated from each repeating earthquake sequence. Black circles and dots represent hypocenters based on KOERI catalogue. Red square is the location of a seafloor acoustic ranging station by Yamamoto et al. (2019).

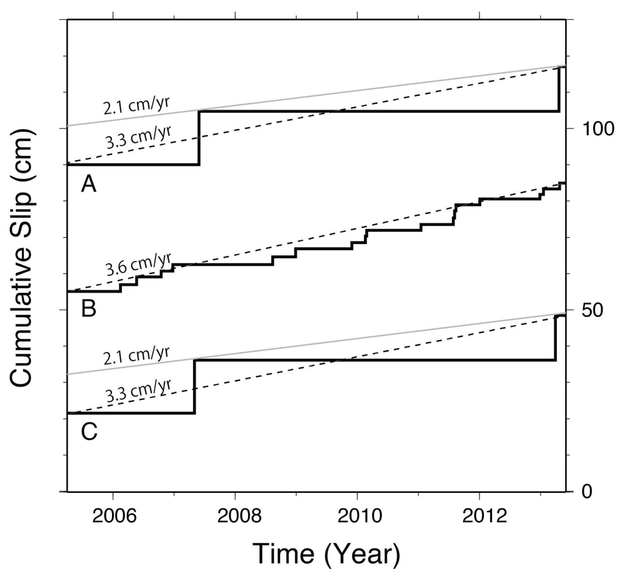

Fig. 5. Cumulative slip of repeating earthquakes in regions A to C. For region B, the cumulative slips are averaged for 7 sequences. The dashed line show slip rate when considering all observation period. The gray lines in regions A and C show the rate considering for the time period between two events.

3. Earthquake relocation and the depth extent of the fault slow slip in the Sea of Marmara

The repeating earthquakes in region B are located under the Sea of Marmara and the depth constraint on the events can be poor due to the lack of nearby stations (Yamamoto et al., 2017). To constrain the depth extent of the repeaters that indicate the location of fault slow slip, we conducted relative hypocenter determinations of 17 repeating earthquakes in region B with another 96 regular earthquakes whose locations were constrained by Ocean Bottom Seismometer (OBS) data and commonly listed in KOERI's earthquake catalogue (Yamamoto et al., 2017; hereafter, “OBS events”).

First, we added the arrival time data for the 96 OBS events at 49 land stations from KOERI's catalogue to the original arrival time dataset (Yamamoto et al., 2017). Then, we merged the arrival time dataset of the 96 OBS events with that of the 17 repeaters and calculated the double-difference data for event pairs whose hypocentral separations were < 20 km. We also established an extended three-dimensional (3-D) velocity structure by combining the offshore 3-D velocity model (Yamamoto et al., 2017, Figs. 6c, S1) with KOERI's 1-D velocity model (Kalafat et al., 1987, Fig. S1) for the onshore area. Since we assumed a simple velocity model for the onshore area, the difference with actual velocity structure may arise mislocation in the hypocenters. To avoid this issue, we calculated the station correction values for travel time data at land stations obtained by the average of travel time residuals of the 96 OBS events, assuming that the locations of the OBS events (Yamamoto et al., 2017) were correct. We applied the tomoFDD code (Zhang and Thurber, 2006) for this relocation, using both absolute travel time data and double-difference data at the 49 land stations and 15 OBS stations (Figs. 2 and 6). This procedure allowed us to link repeaters and OBS events through double-difference data for land stations, and we could relocate repeaters reflecting part of the information of the OBS, although it is indirect. The estimation errors of most of the repeaters are < 3 km and 5 km in the horizontal and vertical directions, respectively.

The results show that the repeaters in region B are located at 10–20 km depth along ~40 km segment of the NAF (Fig. 6). By the relocation, the earthquakes that was located shallow (< 10 km depth) became deeper. The earthquakes that were located western side also shifted to east. The relocated hypocenters show that there is a seismic gap at longitude 27.5 to 28.0 in the depth range of 0–10 km. At the longitude of 28.0 to 28.75, the seismicity becomes shallow to the east. The repeating earthquakes are located within the seismicity in the longitude from 27.75 to 28.25. We again do not see spatial pattern of slip rates from the relocated hypocenters.

4. Discussion

4.1. Creep rate in the Sea of Marmara

We found the repeating earthquake sequences in the western portion of the Sea of Marmara (WH and CB) show slip rates of 3.3–5.7 cm/yr, which is comparable or even greater than the relative plate motion between Eurasian and Anatolian plates (~2.4 cm/yr, Sella et al., 2002). One possibility for a slip rate that is faster than the plate rate is the estimation error of the earthquake magnitude which is estimated by KOERI. However, we don't have enough information on the systematic magnitude shift on the KOERI's catalogue. The other possibility for a slip rate that is faster than the plate rate and is considered mainly accommodated by NAF is the small number of repeating earthquakes in our study period (2 to 3). If there was spatio-temporal change of slip rate in the study area, only the area and timing that showed a fast slip rate can be sampled. Spatio-temporal changes of slip rates are observed in many plate boundaries (e.g., Nadeau and McEvilly, 2004; Uchida et al., 2016). Therefore, the slip rates estimated in this study may represent the upper limit of the slip rate.

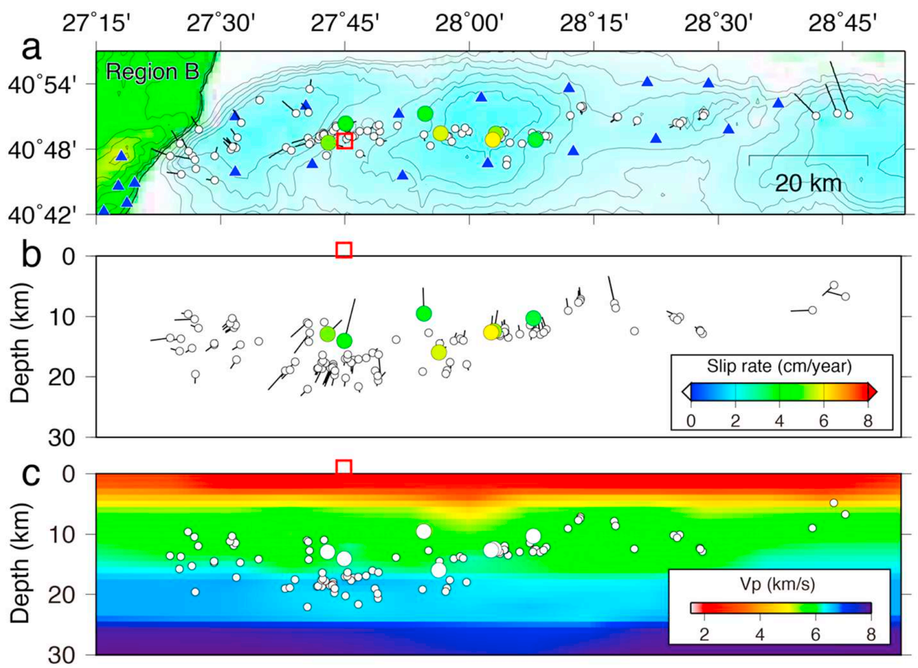

Fig. 6. Relocated hypocenters for region B. (a) and (b) Large circles color coded by slip rate show the locations of repeating earthquake sequence. White circles show background earthquakes that occurred during the period of the OBS observation. Black lines connect original and relocated hypocenters. The red square is the location of a seafloor acoustic ranging station by Yamamoto et al. (2019). Blue triangles show seismic stations used for the earthquake relocation. (c) Relocated hypocenter location with 3D P-wave velocity structure along 40.8°N used for the relocation.

In the western portion of the Sea of Marmara, the existence of repeating earthquakes and fault creep are also suggested by Schmittbuhl et al. (2016) and Bohnhoff et al. (2017). One of the two repeating earthquake sequences found by Bohnhoff et al. (2017) corresponds to sequence 2 (Table 1) identified in our study. The repeating earthquakes found by Schmittbuhl et al. (2016) contain more smaller events and are located in the eastern part of group B. In terms of the estimated coupling ratio, their results are different from our study, which indicated nearly ~0% coupling, while Schmittbuhl et al. (2016) suggest a coupling ratio of > 90% and Bohnhoff et al. (2017) suggest 25–75% (Table 2). Please note that we defined the coupling ratio C = 1 − (repeater slip rate / long-term plate rate). Schmittbuhl et al. (2016) suggest if the slip of all 9 repeating sequences are added the slip-rate becomes close to the long-term plate motion, but we think there is no reasonable justification to add slips from different repeater sequences. We think the discrepancy between our study and the previous two studies mainly originated from the estimation method (scaling) of slip from each earthquake (Table 2). In our study, we used Nadeau and Johnson's scaling relationship (Eq. (1)), while on the other hand, Schmittbuhl et al. (2016) used spectral analysis and Bohnhoff et al. (2017) used a standard scaling relationship between earthquake size and slip assuming a stress drop. It is known that Nadeau and Johnson's relationship tends to give larger slip for small earthquakes (Nadeau and Johnson, 1998). The difference between Nadeau and Johnson (1998)'s scaling relationship and other scaling is discussed extensively in the previous studies (e.g., Nadeau and Johnson, 1998; Sammis and Rice, 2001; Beeler et al., 2001; Chen and Lapusta, 2009). One of plausible explanation is slip during the earthquake cycle of repeating earthquakes (e.g., Beeler et al., 2001; Chen and Lapusta, 2009). Such aseismic slip can explain the discrepancy between Nadeau and Johnson (1998)'s and standard scaling relationships. To confirm the applicability of the Nadeau and Johnson (1998)'s scaling relationship to this area, we need independent observation of creep to calibrate it at the same location which is not available now. However, the relationship specialized for repeating earthquakes is applied in many fault zones (e.g., Chen et al., 2008; Materna et al., 2018; Uchida et al., 2003) and in good agreement with geodetic data inversions (e.g., Chaussard et al., 2015; Nomura et al., 2016). Therefore, we consider Nadeau and Johnson's relationship to be good at estimating fault creep in this study, but if we had used a standard scaling relationship by assuming a stress drop of 10 MPa, the slip rates become 4.4–14 mm/yr, which are comparable with other studies (Table 2).

4.2. Spatial distribution of coupling in the Sea of Marmara

The hypocenter relocation of repeating earthquakes in the Sea of Marmara shows that most of these were located deeper than 10 km and that the seismicity including repeaters becomes shallow to the east. The sea bottom acoustic ranging observations conducted by Yamamoto et al. (2019) were located just above the repeater sequences (Fig. 6, squares), and suggest partial locking in the depth range of 0–8 km, full locking in the depth range of 8–11 km, and decoupling at depths below 11 km. Our repeater distribution of deeper than ~10 km and estimated coupling of ~0% at those depths is consistent with their results. The rupture area of the 1912 Murefte-Sarkoy (Ganos) earthquake occurs to the west of the repeater distribution. The seismicity, including repeaters, may be delineating the deeper limit of the locked area because repeating earthquakes and slow slip often occur in the transitional area between locked and aseismic areas with full creep (e.g., Bürgmann et al., 2000; Uchida and Matsuzawa, 2011). Fig. 7 schematically depicts the distribution of the repeating earthquakes and locked area. To the east of ~28° E, the seismicity and transitional zone become shallower, suggesting the area of full creep extends to shallower depths. The Sea of

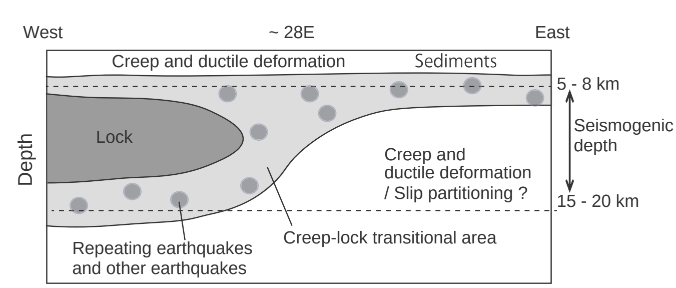

Fig. 7. Schematic diagram showing the distribution of repeating earthquakes and interplate coupling. The repeating earthquakes have greater depth to the west and shallower depth to the east. The deep repeater to the west of 28E probably delineate the locked area for the 1912 earthquake. The limitation of seismicity and repeating earthquakes to shallow depths suggest less coupling or slip partitioning at depth.

Marmara is a large pull-apart system (Fig. 1) that includes smaller segments, and is in a transtensional tectonic regime (Armijo et al., 2002). Actually, both strike-slip and normal faulting earthquakes are occurring in the Sea of Marmara (e.g., Nakano et al., 2015; Pınar et al., 2016). However, no net opening is observed across the sea perpendicular to the fault trace, suggesting slip partitioning is occurring in the Sea of Marmara (Flerit et al., 2003). Yamamoto et al. (2017) suggest the fault in the eastern part is not vertical and dips to the south. Therefore, slip partitioning by multiple faults may be playing an important role in the deformation in the eastern part.

5. Conclusion

We searched for repeating earthquakes in and around the Sea of Marmara from the waveform similarities of earthquakes recorded by permanent stations from 2005 to 2013. The repeating earthquakes were located along the NAF and three clusters of activities were confined near the segment boundaries of previous $M > 7$ earthquake ruptures. The repeating earthquake clusters, including the most active cluster in the western portion of the Sea of Marmara, show slip rates of 3–4 cm/yr, suggesting weak coupling there. Hypocenter relocation using data from an ocean bottom seismometer was conducted after the repeating earthquake analysis and contributed to constraining the depths of the repeating earthquakes (depth $\geqq 10$ km) using a three dimensional velocity structure and double-difference data. Considering the repeating earthquake analysis results (this study), the acoustic-ranging determined creep rate (Yamamoto et al., 2019), and pre-existing geodetic data, interplate coupling in the Sea of Marmara is not uniform and has strong spatial variations.

Supplementary data to this article can be found online at https://doi.org/10.1016/j.tecto.2019.228185.

Funding

This work is supported by the Japan International Cooperation Agency, Japan Science and Technology Agency, the Ministry of Development of Turkey, and Japan Society for the Promotion of Science.

Acknowledgements

The waveform data used in this study were provided by Bogazici University Kandilli Observatory and Earthquake Research Institute (KOERI). The KOERI data service is funded by the Ministry of Development of Turkey through the instrumentation and operation of the nationwide seismic network (https://doi.org/10.7914/SN/KO). This work is supported by the Marmara Disaster Mitigation (MarDIM) project, formally known as the "Earthquake and Tsunami Disaster Mitigation in the Marmara Region and Disaster Education in Turkey" project and JSPS KAKENHI 15K05260, 16H06473, 17KK0081. We are grateful to Y. Kaneda, Y. Honkura, S. Çitak, and N. Takahashi for their help collecting data and supporting this joint research through the MarDIM project. We thank S. Baris and anonymous reviewer for their helpful comments, which improved the manuscript very much. All the figures in this paper were plotted using the GMT software package (Wessel and Smith, 1995).

References

Aksoy, M.E., Meghraoui, M., Vallée, M., Çakır, Z., 2010. Rupture characteristics of the A.D. 1912 Mürefte (Ganos) earthquake segment of the North Anatolian fault (western Turkey). Geology 38, 991–994.

Ambraseys, N., 2002. The seismic activity of the Marmara Sea region over the last 2000 years. Bull. Seismol. Soc. Am. 92, 1–18.

Armijo, R., Meyer, B., Navarro, S., King, G., Barka, A., 2002. Asymmetric slip partitioning in the Sea of Marmara pull-apart: a clue to propagation processes of the North Anatolian Fault? Terra Nova 14, 80–86.

Barka, A., et al., 2002. The surface rupture and slip distribution of the 17 August 1999 Izmit earthquake (M 7.4), North Anatolian fault. Bull. Seismol. Soc. Am. 92, 43–60.

Beeler, N.M., Lockner, D.L., Hickman, S.H., 2001. A simple stick-slip and creep-slip model for repeating earthquakes and its implication for microearthquakes at Parkfield. Bull. Seismol. Soc. Am. 91, 1797–1804.

Bohnhoff, M., Bulut, F., Dresen, G., Malin, P.E., Eken, T., Aktar, M., 2013. An earthquake gap south of Istanbul. Nat. Commun. 4, 1999. https://doi.org/10.1038/ncomms2999.

Bohnhoff, M., Wollin, C., Domigall, D., Küperkoch, L., Martínez-Garzón, P., Kwiatek, G., Dresen, G., Malin, P.E., 2017. Repeating Marmara Sea earthquakes: indication for fault creep. Geophys. J. Int. 210, 332–339.

Bouchon, M., Toksoz, M.N., Karabulut, H., Bouin, M.-P., Dietrich, M., Aktar, M., Edie, M., 2002. Space and time evolution of rupture and faulting during the 1999 Izmit (Turkey) earthquake. Bull. Seismol. Soc. Am. 92, 256–266.

Bulut, F., Ellsworth W, L., Bohnhoff, M., Aktar, M., Dresen, G., 2011. Spatiotemporal earthquake clusters along the North Anatolian fault zone offshore Istanbul. Bull. Seismol. Soc. Am. 101 (4), 1759–1768.

Bürgmann, R., Schmidt, D., Nadeau, R.M., d'Alessio, M., Fielding, E., Manaker, D., McEvilly, T.V., Murray, M.H., 2000. Earthquake potential along the Northern Hayward Fault, California. Science 289, 1178–1182.

Chaussard, E., Bürgmann, R., Fattahi, H., Johnson, C.W., Nadeau, R., Taira, T., Johanson, I., 2015. Interseismic coupling and refined earthquake potential on the Hayward-Calaveras fault zone. J. Geophys. Res. Solid Earth 120, 8570–8590.

Chen, T., Lapusta, N., 2009. Scaling of small repeating earthquakes explained by interaction of seismic and aseismic slip in a rate and state fault model. J. Geophys. Res. 114.

Chen, K.H., Nadeau, R.M., Rau, R.-J., 2008. Characteristic repeating earthquakes in an arc-continent collision boundary zone: the Chihshang fault of eastern Taiwan. Earth Planet. Sci. Lett. 276, 262–272.

Flerit, F., Armijo, R., King, G.C.P., Meyer, B., Barka, A., 2003. Slip partitioning in the Sea of Marmara pull-apart determined from GPS velocity vectors. Geophys. J. Int. 154, 1–7.

Hanks, T.C., Kanamori, H., 1979. A moment magnitude scale. J. Geophys. Res. 84, 2348–2350.

Kalafat, D., Gürbüz, C., Üçer, S.B., 1987. Investigation of the crust and upper mantle structure in western Turkey. Earthq. Res. Bull. 59, 43–64.

Materna, K., Taira, T.A., Bürgmann, R., 2018. Aseismic transform fault slip at the Mendocino Triple Junction from characteristically repeating earthquakes. Geophys. Res. Lett. 45, 699–707.

McClusky, S., Balassanian, S., Barka, A., Demir, C., Ergintav, S., Georgiev, I., Gurkan, O., Hamburger, M., Hurst, K., Kahle, H., Kastens, K., Kekelidze, G., King, R., Kotzev, V., Lenk, O., Mahmoud, S., Mishin, A., Nadariya, M., Ouzounis, A., Paradissis, D., Peter, Y., Prilepin, M., Reilinger, R., Sanli, I., Seeger, H., Tealeb, A., Toksöz, M.N., Veis, G., 2000. Global Positioning System constraints on plate kinematics and dynamics in the eastern Mediterranean and Caucasus. J. Geophys. Res. Solid Earth 105, 5695–5719.

Nadeau, R.M., Johnson, L.R., 1998. Seismological studies at Parkfield VI: moment release rates and estimates of source parameters for small repeating earthquakes. Bull. Seismol. Soc. Am. 88, 790–814.

Nadeau, R.M., McEvilly, T.V., 1999. Fault slip rates at depth from recurrence intervals of repeating microearthquakes. Science 285, 718–721.

Nadeau, R.M., McEvilly, T.V., 2004. Periodic pulsing of characteristic microearthquakes on the San Andreas Fault. Science 303, 220–222.

Nakano, M., Citak, S., Kalafat, D., 2015. Focal mechanism determinations of earthquakes along the North Anatolian fault, beneath the Sea of Marmara and the Aegean Sea. Earth Planets Space 67, 159. https://doi.org/10.1186/s40623-015-0330-z.

Nomura, S., Ogata, Y., Uchida, N., Matsu'ura, M., 2016. Spatiotemporal variations of interplate slip rates in northeast Japan inverted from recurrence intervals of repeating earthquakes. Geophys. J. Int. 208, 468–481. https://doi.org/10.1093/gji/ggw395.

Parsons, T., 2004. Recalculated probability of M ≥ 7 earthquakes beneath the Sea of Marmara, Turkey. J. Geophys. Res. 109, B05304 (05310.01029/02003jb002667).

Pınar, A., Coşkun, Z., Mert, A., Kalafat, D., 2016. Frictional strength of North Anatolian fault in eastern Marmara region. Earth Planets Space 68, 62. https://doi.org/10.1186/s40623-016-0435-z.

Sakic, P., Piété, H., Ballu, V., Royer, J.-Y., Kopp, H., Lange, D., Petersen, F., Özeren, M.S., Ergintav, S., Geli, L., Henry, P., Deschamps, A., 2016. No significant steady state surface creep along the North Anatolian Fault offshore Istanbul: results of 6 months of seafloor acoustic ranging. Geophys. Res. Lett. 43, 6817–6825.

Sammis, C.G., Rice, J.R., 2001. Repeating earthquakes as low-stress-drop events at a border between locked and creeping fault patches. Bull. Seismol. Soc. Am. 91, 532–537.

Schmittbuhl, J., Karabulut, H., Lengliné, O., Bouchon, M., 2016. Long-lasting seismic repeaters in the Central Basin of the Main Marmara Fault. Geophys. Res. Lett. 43, 9527–9534.

Sella, G.F., Dixon, T.H., Mao, A., 2002. REVEL: a model for recent plate velocities from space geodesy. J. Geophys. Res. 107, 2081.

Şengör, A.M.C., Tüysüz, O., İmren, C., Sakınç, M., Eyidoğan, H., Görür, N., Pichon, X.L., Rangin, C., 2005. The North Anatolian Fault: a new look. Annu. Rev. Earth Planet. Sci. 33, 37–112.

Stein, R.S., Barka, A.A., Dieterich, J.H., 1997. Progressive failure on the North Anatolian fault since 1939 by earthquake stress triggering. Geophys. J. Int. 128, 594–604.

Tibi, R., Bock, G., Xia, Y., Baumbach, M., Grosser, H., Milkereit, C., Karakisa, S., Zünbül, S., Kind, R., Zschau, J., 2001. Rupture processes of the 1999 August 17 Izmit and November 12 Düzce (Turkey) earthquakes. Geophys. J. Int. 144, F1–F7.

Uchida, N., 2019. Detection of repeating earthquakes and their application in characterizing slow fault slip. Prog. Earth Planet. Sci. 6, 40. https://doi.org/10.1186/s40645-019-0284-z.

Uchida, N., Bürgmann, R., 2019. Repeating earthquakes. Annu. Rev. Earth Planet. Sci. 47. https://doi.org/10.1146/annurev-earth-053018-060119.

Uchida, N., Matsuzawa, T., 2011. Coupling coefficient, hierarchical structure, and earthquake cycle for the source area of the 2011 off the Pacific coast of Tohoku earthquake inferred from small repeating earthquake data. Earth Planets Space 63, 675–679.

Uchida, N., Matsuzawa, T., Igarashi, T., Hasegawa, A., 2003. Interplate quasi-static slip off Sanriku, NE Japan, estimated from repeating earthquakes. Geophys. Res. Lett. 30. https://doi.org/10.1029/2003GL017452.
Uchida, N., Matsuzawa, T., Hirahara, S., Hasegawa, A., 2006. Small repeating earthquakes and interplate creep around the 2005 Miyagi-oki earthquake (M7.2). Earth Planets Space 58, 1577–1580.
Uchida, N., Iinuma, T., Nadeau, R.M., Bürgmann, R., Hino, R., 2016. Periodic slow slip triggers megathrust zone earthquakes in northeastern Japan. Science 351, 488–492.
Wessel, P., Smith, W.H.F., 1995. New version of generic mapping tools released. Eos. Trans. AGU 76, 329.
Yamamoto, Y., Takahashi, N., Pinar, A., Kalafat, D., Citak, S., Comoglu, M., Polat, R., Kaneda, Y., 2017. Geometry and segmentation of the North Anatolian Fault beneath the Marmara Sea, Turkey, deduced from long-term ocean bottom seismographic observations. J. Geophys. Res. Solid Earth 122, 2069–2084.
Yamamoto, R., Kido, M., Ohta, Y., Takahashi, N., Yamamoto, Y., Pinar, A., Kalafat, D., Özener, H., Kaneda, Y., 2019. Seafloor geodesy revealed partial creep of the North Anatolian Fault submerged in the Sea of Marmara. Geophys. Res. Lett. https://doi.org/10.1029/2018GL080984.
Zhang, H., Thurber, C., 2006. Development and applications of double-difference seismic tomography. Pure Appl. Geophys. 163, 373–403.